



Integrated Master's Degree in Biomedical Engineering

19<sup>th</sup> May, 2017

**Tissue Biomechanics**

Professors: Paulo Fernandes and Carlos Quental

**BIOMECHANICS ANALYSIS OF THE FEMUR, IN THE  
PRESENCE AND ABSENCE OF A HIP-RESURFACING  
PROSTHESIS, BASED IN THE HUISKES MODEL FOR BONE  
ADAPTATION**

**Manuel Rosado Comenda, 78642**

e-mail: manuel.comenda@tecnico.ulisboa.pt

**Maria Catarina Botelho, 78741**

e-mail: catarina.t.botelho@gmail.com

**João Mocho Ferreira, 78750**

e-mail: j12mocho@gmail.com

**Key-words:**

Huiskes' model, Hip-resurfacing prosthesis, Bone adaptation, MATLAB®, Abaqus®, Finite element method, Stress shielding, Femur, bone densities.

**Abstract:**

The aim of this work is the study of the bone adaptation in a 3D model of a femur, in the presence and absence of a hip-resurfacing prosthesis, with two loading cases, based on Huiskes' model implemented in MATLAB® and using the commercial finite element method software Abaqus®. Among all the Huiskes' model parameters tested, the ones chosen that better represent the reality are:  $k=0.009$ , step size=3 and  $s=0.0$ . The results show the existence of stress shielding phenomenon in bone epiphysis when a prosthesis is applied while the only change in bone's diaphysis was the increase of the medullar cavity volume. Considering materials with elastic modulus above 17 GPa there is not significant differences in the results, i.e., stress shielding is present but it does not suffer changes depending on the material used, except the case of a material with Young's modulus of 3 GPa that is was also tested to simulate a material with similar properties of trabecular bone that exists in bone epiphysis.

## Contents

I.	Introduction.....	1
I.1.	Problem description .....	1
II.	Theoretical fundamentals .....	2
II.1.	Long bones: tissue and anatomy.....	2
II.2.	Bone adaptation and the Huiskes' model .....	3
III.	Methodology .....	4
III.1.	Geometric modulation (SolidWorks®).....	4
III.2.	Finite-element method in Abaqus®.....	5
III.3.	Convergence analysis .....	6
III.4.	MATLAB® implementations of the Huiskes' model for bone remodelling .....	7
IV.	Results .....	8
IV.1.	Analysis of the intact bone and definition of the Huiskes' model parameters .....	8
IV.2.	Analysis of the bone with the insertion of a hip-resurfacing prosthesis .....	10
V.	Discussion.....	11
VI.	Conclusion .....	13
VII.	References:.....	14
VIII.	Appendix.....	15
A.	MATLAB® implementations of the Huiskes' model for bone remodelling .....	15
A.1.	Script for the intact bone: bone.m.....	15
A.2.	Script for bone with implant: prosthesis.m .....	17
A.3.	Convergence of the distribution of densities for the intact bone .....	19
B.	Results from simulations done for searching the Huiskes' model parameters .....	20
C.	Results from simulations done for the different hip-resurfacing prosthesis' materials.....	21
D.	Results from colleagues for comparison .....	24

## I. Introduction

The objective of this project is to implement a model for bone adaptation following Huiskes' model, using the Finite Element Method in *software Abaqus*® for the simulation of the energy strain density ( $U$ ), using *SolidWorks*® for drawing the components and using *MATLAB*® to calculate the actualizations of densities ( $\rho$ ) and for the interface. The study aims to understand the differences in bone resorption between a healthy femur and a femur with a hip-resurfacing prosthesis, and how this difference conditions the bone density.

The bone loss caused by the introduction of an implant is an issue of major importance, once it can lead to the premature failure of the implant. This will condition the patient's life quality, once the patient needs to undergo a new surgery and does not have enough bone mineral density to fix the new implant [1].

Bone loss is mainly caused by two factors: particle wear and stress shielding [1]. Stress shielding is caused by the stiffness differences between the bone and the implant [2]. In this way, this project intends to study different prosthesis materials to compare the differences in bone adaptation.

### I.1. Problem description

The problem under this study concerns a femur in two different situations: the intact femur, and a femur with a non-cemented hip-resurfacing prosthesis, see Figure I.1.1 It is considered that the prosthesis is totally osteointegrated within the bone. The properties of the material are presented in Table I.1.2. Besides the Co-Cr and the iso-elastic case proposed, it was also made a comparative analysis for materials such as stainless steel and titanium, whose properties are also presented Table I.1.2.



Figure I.1.1. X-RAY image of a hip-resurfacing prosthesis inserted in a right femur.

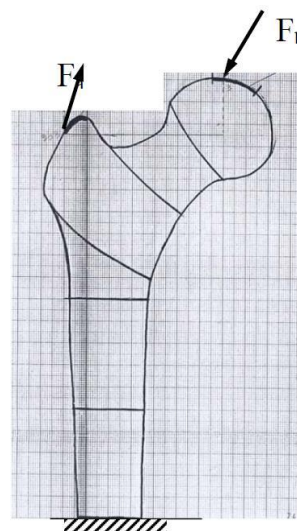


Figure I.1.2. femur schematics with the representation of the forces applied.

*Table I.1.1. Young's modulus and Poisson coefficient of compact bone and the prosthesis.*

	E (GPa)	$\nu$
Compact bone	17 <sup>1</sup>	0.3
Prosthesis - Co-Cr	130	0.3
Prosthesis – “isoelastic material”	17	0.3
Prosthesis – titanium alloy [1]	114	0.3
Prosthesis – stainless steel [3]	200	0.3

There are two loading cases considered, gait and climbing stairs, and the forces applied in both cases to the femur are represented in Figure I.1.2 and Table I.1.1.

*Table I.1.2. Forces applied in the femur, as represented in Figure I.1.2.*

Loading situations	Loads	$F_x$ (N)	$F_y$ (N)	$F_z$ (N)
Gait	$F_h$	-224	-2246	972
	$F_a$	768	1210	-726
Climbing stairs	$F_h$	457	-1707	769
	$F_a$	383	547	-669

## II. Theoretical fundamentals

### II.1. Long bones: tissue and anatomy

The bone macrostructure is the most important level for understanding bone's mechanical properties. According to the macrostructure, there are two main types of bone tissue: compact bone and cancellous or trabecular bone. Compact bone is solid, with few spaces in it, only for blood, canaliculi, osteocytes and erosion cavities [4]. All the osteons in compact bone are aligned in the same direction, making it strong when stressed in the axis of this alignment [5]. The cancellous bone is characterized by larger spaces [4]. It consists of a network of struts and plates covered by a thin layer of compact bone. Cancellous bone is found where bones are not heavily stressed or where stress arrives from many directions. The trabeculae are oriented along stress lines. Cancellous bone is much lighter, reducing the total weight of the bones, and making it easier for the muscles to move them [5].

Long bones are characterized by an extended tubular shaft, the diaphysis, and epiphysis, the round expanded ends of the diaphysis, which are part of the articulation with other bones. The diaphysis is connected to each epiphysis at a narrow zone called metaphysis. The wall of the diaphysis is made of compact bone, with a medullary cavity in the middle. The epiphysis is mainly made of cancellous bone, with a very thin layer of compact bone in the surface of some regions [5]. This structure is visible for the femur in Figure II.1.1.

<sup>1</sup> In the simulation, it is not assumed that the bone has  $E=17$  GPa in all of its volume, the young's modulus is dependent on the density, as it will be explained in section II.2.

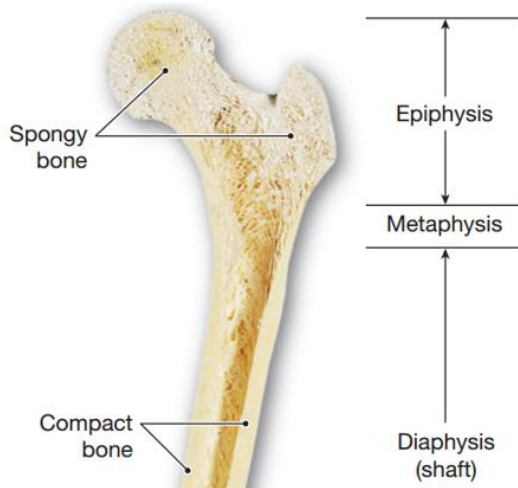


Figure II.1.1 femoral macrostructure [5]

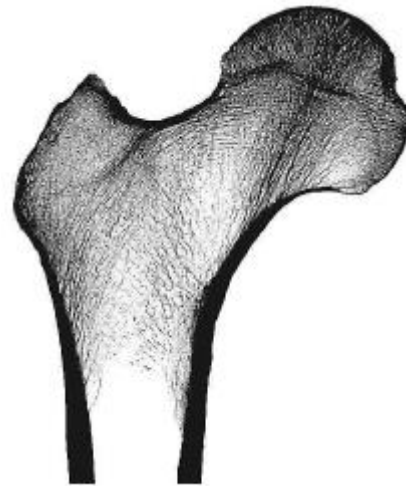


Figure II.1.2. CT scan of femur's epiphysis, which emphasizes the differences in bone density [6].

## II.2. Bone adaptation and the Huiskes' model

Generally, bone adaptation can be defined as a change in bone structure (trabeculae orientation, bone density and bone surface density) as a response to mechanical stimuli and physiological mechanisms [6]. Bone remodelling is a continuous turnover between bone resorption (activity of osteoclasts) and bone formation (activity of osteoclasts). [7]

According to Wolf's Law, bone remodelling comprises three important aspects: optimization of bone strength with respect to the weight, trabeculae aligns with principal stresses directions and the cell mediated self-regulation of bone responds to mechanical stimulus, namely strain, stress and strain energy density [6].

Huiskes' model is one of the several mathematical models existent to describe bone adaptation. It considers that bone is an isotropic material and elastic strain energy density is the mechanical stimulus, which is given by equation 1. The model is graphically represented in Figure II.2.1.

$$U = \frac{1}{2} \sigma_{ij} \epsilon_{ij} \quad (1)$$

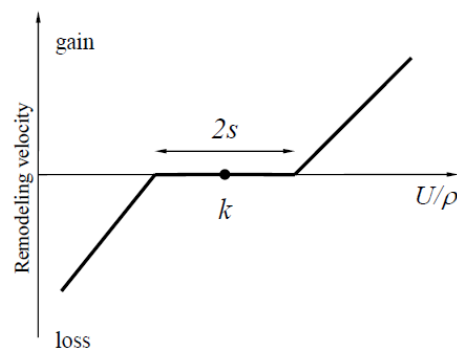


Figure II.2.1 Graphical representation of the Huiskes' model. [6]

In Figure II.2.1, the plateau defines a range of strain density energy where the mechanical stimulus is null. The length of this region is  $2s$ .

The evolution of the internal bone adaptation is described in equation (2), and computationally it is solved using a forward Euler method, presented in equation (3).

$$\frac{d\rho}{dt} = \begin{cases} B\left(\frac{U}{\rho} - (1-s) \cdot k\right), & \text{if } \frac{U}{\rho} < (1-s) \cdot k \\ 0, & \text{otherwise} \\ B\left(\frac{U}{\rho} - (1+s) \cdot k\right), & \text{if } \frac{U}{\rho} > (1+s) \cdot k \end{cases} \quad (2)$$

$$\rho_{t+\Delta t} = \begin{cases} \rho_t + \Delta t \times B\left(\frac{U}{\rho} - (1-s) \cdot k\right), & \text{if } \frac{U}{\rho} < (1-s) \cdot k \\ \rho_t, & \text{otherwise} \\ \rho_t + \Delta t \times B\left(\frac{U}{\rho} - (1+s) \cdot k\right), & \text{if } \frac{U}{\rho} > (1+s) \cdot k \end{cases} \quad (3)$$

In which  $\Delta t \times B$  refers to the step size. Step size,  $s$ ,  $k$  (metabolic cost of bone formation) and the number of iterations should be chosen conveniently according to the problem.

For multiple loads, which is the case in this study,  $U$  is the average of the  $U$  for each load.

The Young's modulus is defined by equation (4), where  $E$  is given in MPa and  $\rho$  between  $0.1\text{g/cm}^3$  and  $0.74\text{g/cm}^3$ .

$$E = 3790 \times \rho^3 \quad (4)$$

### III. Methodology

#### III.1. Geometric modulation (*SolidWorks*®)

The graphical modulation of both the hip-resurfacing prosthesis (Figure III.1.1) and the femur were made in *SolidWorks*®. The femur model was available in the internet [8], then it was cut in *SolidWorks*® with a plane in the diaphysis (Figure III.1.2). The hip-resurfacing prosthesis was elaborated according to the problem proposed and to the surgical technique [9].

The dimensions of the prosthesis are 50 mm for the outer diameter and 36 mm for the inner diameter of the head, 7 mm for the diameter of the stem and 55 mm for the length of the stem.

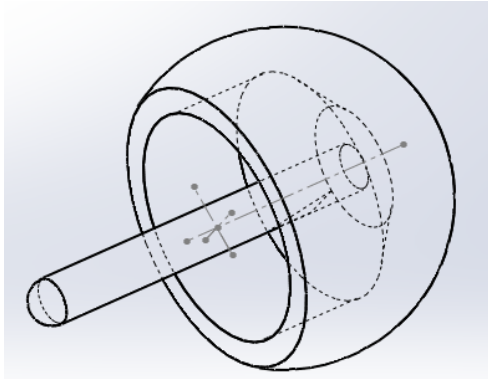


Figure III.1.1. Hip-resurfacing prosthesis made in SolidWorks®.

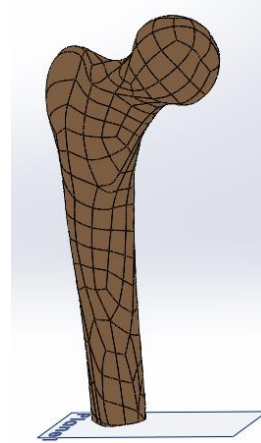


Figure III.1.2. 3D model of femur from [8].

The prosthesis was placed in the correct position in the femur, and both the femur and the assembly of the femur and prosthesis were saved in *ACIS.sat* format, to allow the importation to *Abaqus*®.

### III.2. Finite-element method in *Abaqus*®

The commercial software *Abaqus*® was used to apply the finite element method, to obtain the *von Mises* stresses, the deformations and the energy strain density, and to visualize the results.

The femur and the assembly of the femur and prosthesis were imported to *Abaqus*® as parts. In the following text, the modulation steps will be described for the femur plus prosthesis. The modulation for the intact femur is similar, considering that some steps are not necessary.

The materials for the bone and implant were created and assigned to the two parts. The bone material is isoelastic, the Poisson coefficient is  $\nu=0.3$ , and the Young's modulus is density dependent, according to equation (4), for densities between  $\rho=0.1 \text{ g/cm}^3$  and  $\rho=0.7 \text{ g/cm}^3$ . The bone implant properties were defined as indicated in Table I.1.1.

After, the parts bone and implant were assembled. Since the parts were already in the right position it was only necessary to cut the bone part with the implant, followed by a "geometry merge" with "retain Intersecting Boundaries" in order to have both the materials in one instance to simulate the case of an osteointegrated implant.

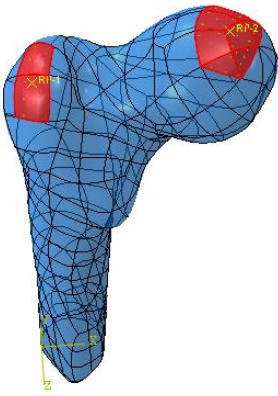


Figure III.2.1. Image of the femur presenting the regions to force application.

The forces were defined uniformly in a region by applying a concentrated force in the centroid of the surfaces chosen (Figure III.2.1) and using the interaction “Coupling”. Two loading cases, gait and climbing stairs, were defined by two different steps and in each one of them the correspondent loads were applied. It is important to create a predefined field “Temperature” and to choose, in field output, “All magnitudes” and “Nodal temperatures”, to assure density dependence of bone material properties and to allow the visualization of densities in all nodes.

A sensitivity analysis, described in the next section, was made to choose the more appropriate mesh seed. After, one “job” was created and submitted.

### III.3. Convergence analysis

To assure the reliability of the results, it is necessary a convergence analysis of the mesh. It was made a simple analysis only for the femur without a prosthesis, in two points (Figure III.3.1), with tetrahedral elements, quadric and linear. (Figure III.3.2 and III.3.3). The use of hexagonal elements was not possible due to the irregular geometry.

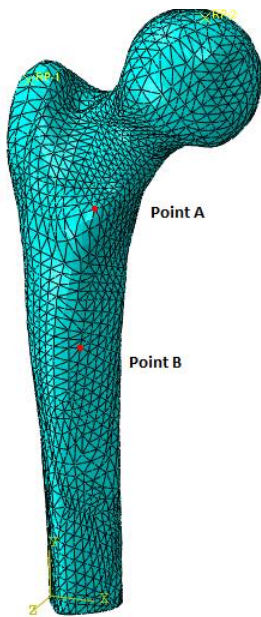


Figure III.3.1 Image of the femur with the points (A and B) chosen for the convergence analysis represented, with seed mesh equal to 4.3mm.

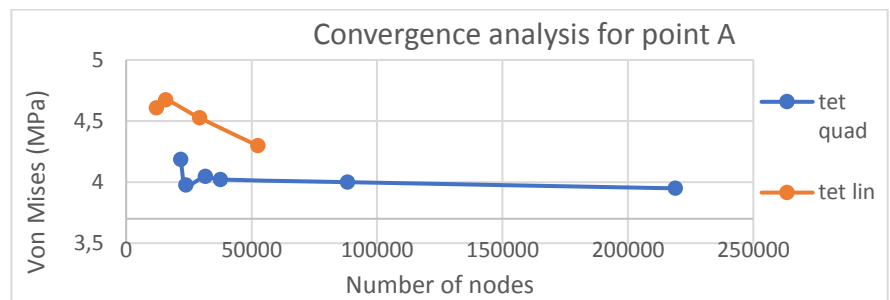


Figure III.3.2 Convergence analysis in point A, for linear (tet lin) and quadratic (tet quad) tetrahedral elements. The dots in the linear elements correspond, from left to right, to a general seed of 3 mm, 2.5 mm, 2 mm and 1.5 mm, under which the computational time was not viable. For the quadratic elements, the dots correspond, from left to right, to 6mm, 5mm, 4.3mm, 4mm, 3mm, and 2mm.

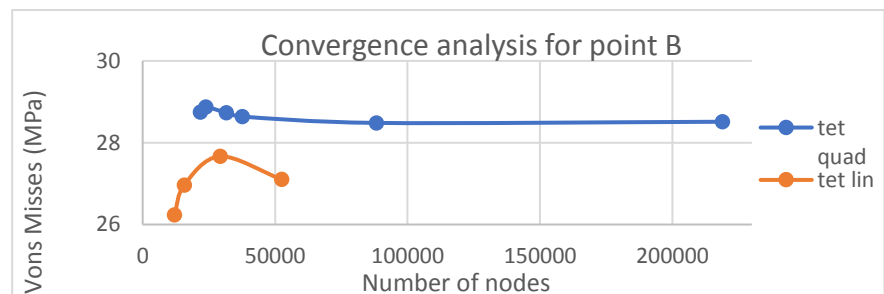


Figure III.3.3 Convergence analysis in point B, for linear (tet lin) and quadratic (tet quad) tetrahedral elements. The dots in the linear elements correspond, from left to right, to a general seed of 3 mm, 2.5 mm, 2 mm and 1.5 mm, under which the computational time was not viable. For the quadratic elements, the dots correspond, from left to right, to 6 mm, 5mm, 4.3 mm, 4 mm, 3 mm, and 2 mm.



Considering the figure III.3.2 and III.3.3, the mesh chosen was of tetrahedral quadratic elements, with general seed of 4.3mm, which represented the best compromise between the convergence of the results and the computation time. The analysis of the linear elements was not explored further, because, for the same number of nodes chosen in the quadratic elements, the linear elements were not yet converging.

#### III.4. MATLAB® implementations of the Huiskes' model for bone remodelling

To use *MATLAB*® for running the Huiskes' model, it was required to open the *Abaqus*® *ODB* file generated after running the Job so it was possible to choose the options “*Unique Nodal*” and “*SENER* (Strain Energy densities)” to the *RPT* file (*ODB* output). After this, the extension of the file *RPY* was changed to *PY* so *MATLAB*® could run it. This had to be made to both the loading cases, gait and climbing stairs. Inside *INP* file, it was replaced the input of the temperature field by an instruction that leads the *Job* to get this information in the file *dens.dat*.

In *MATLAB*®, two *M* files were made, one for intact bone and the other for the bone with the prosthesis implanted, which are presented in Appendix A. Each *M* file is a script (Appendix A.1 and A.2) with two main sections: one where the initial conditions and the inputs, such as the number of nodes, *k*, *s*, *step* and the maximum number of iterations are initialized, and another with a for loop where the *Abaqus*® software is ran, the output energies are read and the new densities are calculated and updated.

As inputs, the script receives an integer of maximum iterations, *niter*, a value for metabolic cost of bone formation, *k*, a value for the *s* and a step size, *step*. Other initial variables are also stated, such as the number of nodes (31502 nodes for bone and 44675 nodes for bone with prosthesis), the initial bone nodal densities matrix, *dens* ( $0.3 \text{ g.cm}^{-3}$ ) and a matrix *previousdens*, where, in each iteration, the densities of the previous iteration are saved to compare with the actual densities, to study its convergence.

After stating the initial conditions, before the loop starts, the stopping condition is verified. If the mean of the absolute value of the difference between the matrices *dens* and *previousdens* is less than  $10^{-3}$ , the loop breaks, otherwise the file *dens.dat* is created/updated with the information within the *dens* matrix. The evolution of the convergence criteria for the chosen parameters is presented in Appendix A.3.

Then, *MATLAB*® runs an *Abaqus*® *Job* through the *INP* file and, after this, it runs a *PY* file for each step that correspond to each loading case. This generates two *RPT* files, where the new nodal Strain energy densities are registered.

Strain energy densities from the *RPT* file of the gait case are read to matrix *ener1* and the ones of the climbing stairs case are read to matrix *ener2*. Then, it is done the mean to these matrices, creating matrix *ener*. When studying bone with prosthesis, the number corresponding to each node is also registered in matrix *ener*, so the algorithm knows what are the nodes which density must be updated (bone nodes).

Huiskes' model, presented in section II.2, was applied to data within *ener* matrix, updating dens matrix. After this, the loop restarts, comparing the new *dens* matrix to *previousdens* and updating this one.

## IV. Results

### IV.1. Analysis of the intact bone and definition of the Huiskes' model parameters

The density analysis of the intact bone was made for different values of *k*, *step size*, *s* and *initial densities*, to model the bone as similar as possible with the reality. Several simulations were made and the most relevant tests are described in table IV.1.1 and figures IV.1.1., IV.1.2. and in Appendix B. The tests presented in the table were chosen because they only change one parameter at the time at it becomes easier to analyse its impact.

Table IV.1.1. Huiskes' model parameters tested. The chosen parameters are highlighted.

k	s	Step size	Initial density (g/cm <sup>3</sup> )	Results
0.004	0.3	3	0.3	Figure IV.1.2. a)
0.04	0.3	3	0.3	Figure IV.1.2. b)
<b>0.009</b>	<b>0.00</b>	<b>3</b>	<b>0.3</b>	<b>Figure IV.1.1.</b>
0.009	0.30	8	0.3	Figure IV.4.2. c)
0.009	0.30	0.8	0.3	Figure IV.4.2. d)
0.009	0.30	3	0.3	Figure VIII.B.1. (Appendix B)

To start, the step size was fixed to 3 and the parameter *k* was analyzed, *k*=0.009 was chosen. Then, the step size was analyzed and chosen the value 3. At last, with *k* and step size fixed, simulations were made to find the influence of parameter *s*, and chosen the value 0.0. The figure IV.1.1 represents the several views of the femur with the parameters that best fit the bone adaptation to reality.

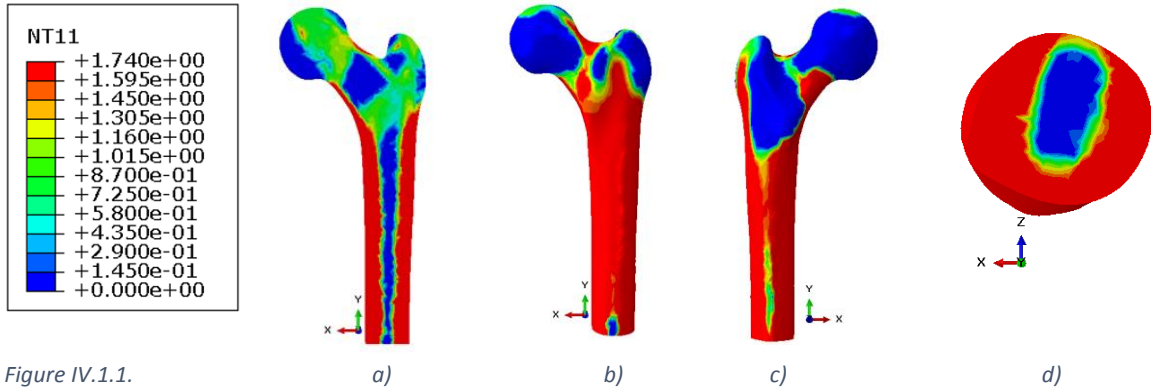


Figure IV.1.1.

These images represent bone density distribution in different cuts and views. Coronal cut in a), transversal in d) and anterior and posterior coronal planes in b) and c). The parameters used are  $k=0.009$ ,  $s=0.0$ ,  $\text{step size}=3$  and  $\text{initial densities}=0.3 \text{ g/cm}^3$ .

In figure IV.1.2. are presented four different images, and each represents the reason to discard some set of parameters.

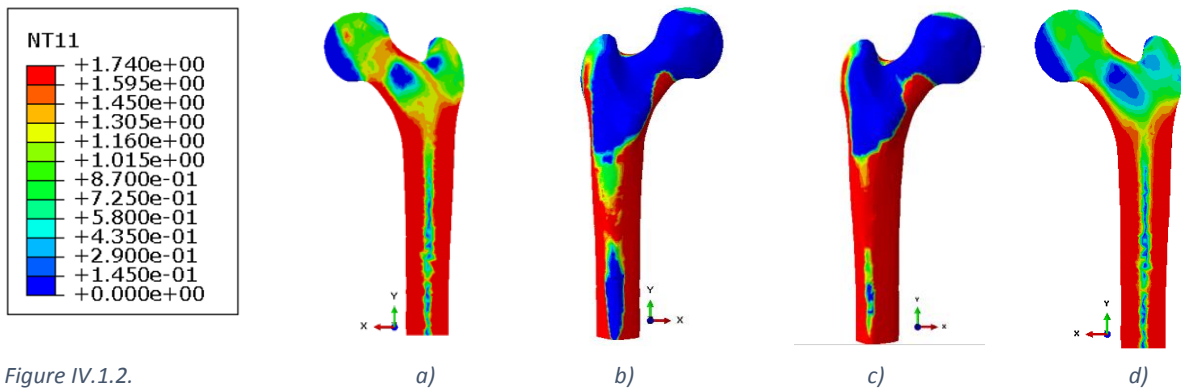


Figure IV.1.2.

These images represent bone density distribution in different cuts and views, with different parameters. Each image demonstrates why some set of parameters were not chose. The parameters used are:  $s=0.3$  and  $\text{initial densities}=0.3 \text{ g/cm}^3$ . a)  $k=0.004$ ,  $\text{step size}=3$  and b)  $k=0.04$ ,  $\text{step size}=3$ ; c)  $k=0.009$ ,  $\text{step size}=8$  and d)  $k=0.009$ ,  $\text{step size}=0.8$ .

Figure IV.1.2. a) was discarded due to the presence of cortical bone in the epiphysis and a non-significant medullar cavity in the diaphysis. Image b) has very low densities in diaphysis' walls, as well as image c). Image d) was excluded due to a non-significant medullar cavity in the diaphysis. To exclude the parameter  $s=0.3$ , Figure VIII.B.5 in appendix B, the only reason was that for  $s=0.0$  there is a more significant medullar cavity in diaphysis.

For a better understanding of the results obtained for densities distribution, in figure IV.1.3 several cuts and views of Von Mises stresses and S13 are presented.

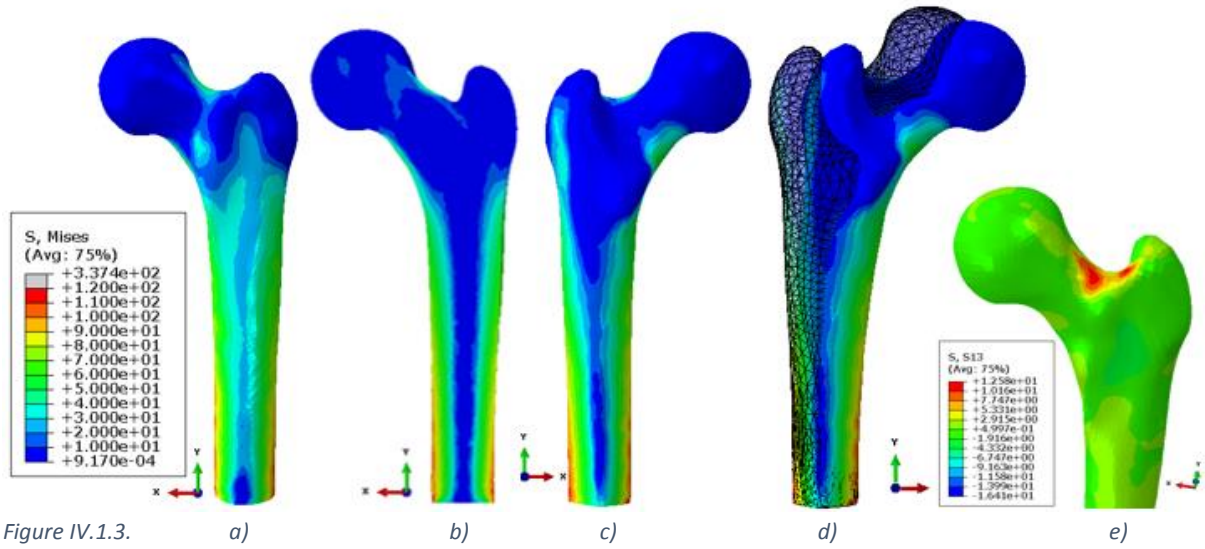


Figure IV.1.3. a) b) c) d) e) Images a) and c) represent Von Mises stresses in undeformed shape and deformed shape in image d), a coronal plane is presented in image b). Image e) represents stresses S13. These images correspond to load case “gate”.

#### IV.2. Analysis of the bone with the insertion of a hip-resurfacing prosthesis

Obtained the Huiskes' model parameters that better fit the reality, the next step was to study the density distribution when a hip-resurfacing prosthesis is implanted. Four different materials were used: Cobalt-chrome, the case with a material  $E=17$  GPa, titanium alloy and stainless steel. The relevant views of the results obtained are presented in figure IV.2.1. and the remaining views in the Appendix C.

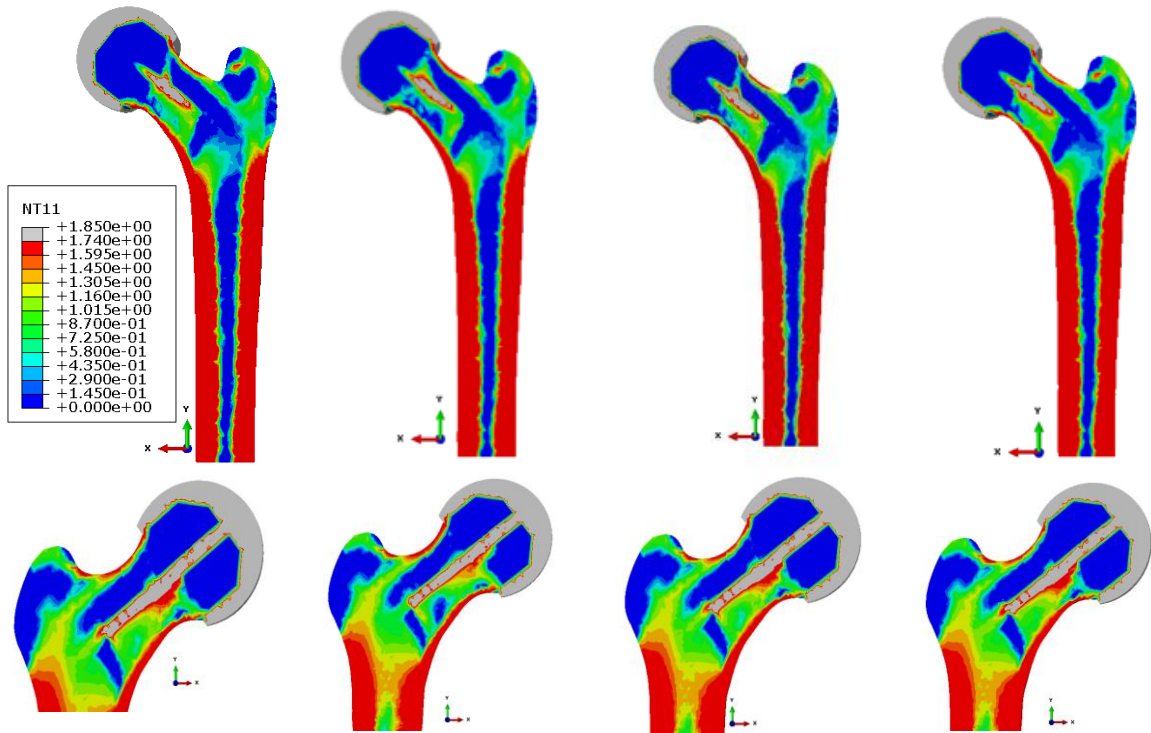


Figure IV.2.1. a) b) c) d) Cuts from coronal plane of bone with hip-resurfacing prosthesis made of different materials. a) Prosthesis of Co-Cr, b) Prosthesis of a material with 17 GPa, c) Prosthesis of titanium alloy and d) Prosthesis of stainless steel. The parameters used are  $k=0.009$ ,  $s=0.0$ , step size=3 and initial densities= $0.3 \text{ g/cm}^3$ .

As the trabecular bone has a Young's modulus of 3 GPa (calculated with equation (4)), a new simulation was made using an implant made of a material with Young's modulus equal to 3 GPa. This simulation was made with the purpose of visualizing bigger differences in the stress shielding phenomenon.

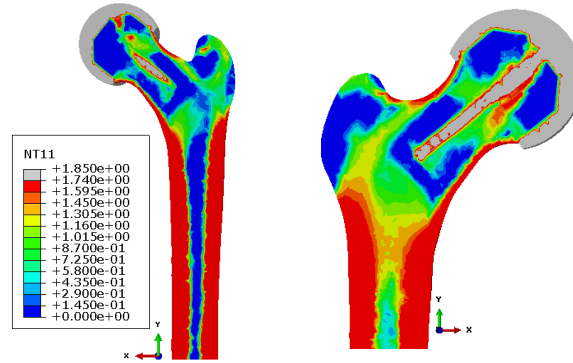


Figure IV.2.2. a) b)  
Cuts from coronal plane of bone with hip-resurfacing prosthesis made of a material with 3 GPa.

## V. Discussion

The mesh obtained is not ideal, nor in matters of convergence (Figures III.3.1 and Figure III.3.2), neither in its geometric configuration. The geometric configuration could be improved if we had drawn the femur model ourselves, and by remaking the partitions in the *Abaqus* software. To improve the convergence, it would be required a more refined mesh, and therefore, more powerful computers that were not available for this project.

Regarding the tests made for the choice of the parameters for the Huiskes' model, it is noticeable that for higher values of  $k$  (namely  $k=0.04$ , Appendix B, Figure VIII.B.2), the medullar cavity is bigger and better defined with densities close to zero, however, the downside is that appears a region on the diaphysis' walls where the densities are also very low, where it should be compact bone (Figure IV.1.2 b)). Besides, in the epiphysis the densities become very low instead of the medium densities representing the trabecular bone that should be found. Using high values for the step size, namely step size=8, also contributes to this phenomenon, as it is visible in Figure IV.1.2.c) and Appendix B, Figure VIII.b.3.

On the other hand, when using low values for  $k$ , the main reason for exclusion is the fact that the medullar cavity disappears, having too high densities (Figure IV.1.2.a and more details in Appendix B, Figure VIII.B.2). Besides, it is also visible the presence of more compact bone within the epiphysis. Using a small value for the step contributes to decrease the dimension of the medullar cavity (Figure IV.1.2.d)).

Concerning the  $s$  parameter, its consequences are not very significant, although it is noticeable that in the epiphysis, for  $s=0.0$ , the medullar cavity is better defined (Figure IV.1.1), when compared to the results for  $s=0.3$  (Appendix B, Figure VIII.B.5).

Considering all these factors, the parameters chosen reflect a compromise that tries to describe the anatomy and macrostructure of a real bone (Figure II.1.1), sacrificing slightly the diameter of the diaphysis, but guaranteeing that the wall of the diaphysis is made of compact bone and the intermediate density of the epiphysis that correspond to the trabecular bone. It is noticeable that the orientation of this region corresponds to the orientation of the applied force  $F_h$ , similarly to what is observed in the femur's CT scan – Figure II.1.2. These results corroborate with the literature, as Astrid Liedert and her colleagues state that “mechanical loading enhances bone formation and directs the newly formed bone along the local loading directions” [9].

The distribution of densities reflects the bone remodelling phenomenon which is conditioned by the stresses distribution along the bone [2]. In this way, it is presented in Figure IV.1.3 the distribution of von Mises stresses, where it is visible that the regions of maximum stresses correspond to the regions of maximum density and vice-versa. Considering, for example, the medullar cavity, which has minimum density, has very little Von Mises stresses; also the region of the diaphysis where the density is not maximum corresponds to a region where the Von Mises stresses are low. Besides, bone cells responsible for bone remodelling respond to local strains engendered in their neighbourhood [9].

It is important to refer, in the context of the analysis of the intact bone, that the obtained model is not totally coherent with the reality, as it always happens with computational models. In this particular situation, some of the reasons that stand out are the fact that it is considering only two forces and two loading cases which is a very simplified version of the loadings that a real bone is subjected to. Besides, there are the reasons already pointed out related to the mesh choice; and the fact that anatomic structures have slightly different geometries from person to person, which can explain some variability in the results.

When the implant is introduced in a bone, it is expected to observe a phenomenon designated stress shielding, which is the osteopenia caused by the reduction of the typical stresses the bone is subjected to, associated with the insertion of an implant. The osteopenia, or lack of bone density due to insufficient bone remodelling, may lead to the loosening of the prosthetic device and osteoporosis. A main factor in the origin of this problem is the differences in the Young's modulus between the implant and the bone [3].

The results obtained when the implant was inserted corroborate these facts. Comparing the Figures IV.1.1 and IV.1.2, it is visible that, in the epiphysis inside the partial sphere of the prosthesis, the bone density is much lower when the implant is inserted. It is also visible that there is an accumulation of bone density the lower stem rim. These results are coherent with the distribution of von Mises stresses, presented in Appendix C, Figures VIII.C.6 and VIII.C.7, and with the ones found in the literature [10].

Comparing the results obtained for the different implant materials with each other, they are not so distinct as one would expect (Figure IV.2.1). Theoretically, any reduction of the stiffness of the implant used should minimize the stress shielding effect [3], however it was studied materials with a Young's modulus from 17 GPa (Figure IV.2.1. b)) to 200 GPa (stainless steel – Figure IV.2.1. d)), and the differences in the stress shielding effect.

The simulation made for the Figure IV.2.1. b) was made for an implant with a Young's modulus of 17 GPa, to simulate the young's modulus of the bone, and therefore, the result should be more similar to the one obtained for the intact bone. However, the prosthesis is implanted on the epiphysis of the femur, which is made of cancellous bone, whose Young's modulus is about 3 GPa. In this way, it was made a new simulation for an implant with Young's modulus of 3 GPa, which are presented in Figure IV.2.2. In this figure, it is observed that the results are more similar to the intact bone, with less reduction of the cancellous bone density.

Analysing the von Mises stresses, it is possible to see a more evident difference comparing the implants made of materials to simulate bone ( $E=3$  GPa and  $E=17$  GPa) – Figure VIII.C.6 - and the metal implants – Figure VIII.C.7. In the metal implants, it is observed a more significant accumulation of stresses in the stem of the implant, which is coherent to what was expected.

It is relevant to say that the fact that hip resurfacing prosthesis have relatively small dimensions when compared to other femoral prosthesis, and are only in contact with the epiphysis of the femur is an advantage to minimize the stress shielding effect. Comparing the results obtained in this study with the ones obtained by our colleagues [11] for the prosthesis showed in Appendix D, Figure VIII.D.1 , according to what was expected, it is visible a more evident stress shielding effect in their prosthesis. In these perspective, it becomes evident the advantages of the geometry of a hip resurfacing prosthesis.

## VI. Conclusion

Making a computational modulation of the femoral adaptation due to mechanical stimuli, presents several challenges and requires finding a compromise between the parameters chosen to represent the reality. Nevertheless, considering the results obtained for bone density distribution, it was possible to validate the Huiskes' model. The parameters that best suited the problem in study were  $k=0.009$ ,  $s=0.0$ , step size=3 and initial densities of  $0.3 \text{ g/cm}^3$ .

Stress shielding phenomenon was observed when the prosthesis was introduced, due to the differences in the Young's Modulus of the implant and the bone. It was not observed significant differences when comparing the stress shielding caused by implants made of several materials, with Young's modulus between 17 GPa and 200 GPa.

Some aspects that could be improved are the geometry and refinement of the mesh and the geometry of the 3D model of the femur.



## VII. References:

- [1] P. Tavakkoli Avval, S. Samiezadeh, V. Klika, and H. Bougherara, "Investigating stress shielding spanned by biomimetic polymer-composite vs. metallic hip stem: A computational study using mechano-biochemical model," *J. Mech. Behav. Biomed. Mater.*, vol. 41, no. January, pp. 56–67, 2015.
- [2] R. Huiskes, H. Weinans, H. J. Grootenboer, M. Dalstra, B. Fudala, and T. J. Slooff, "Adaptive bone-remodeling theory applied to prosthetic-design analysis," *J. Biomech.*, vol. 20, no. 11–12, pp. 1135–1150, 1987.
- [3] W. Khan, E. Muntimadugu, M. Jaffe, and A. J. Domb, "Focal Controlled Drug Delivery," pp. 45–46, 2014.
- [4] J. Currey, "The Structure of Bone Tissue," *Bones*, p. 25, 2002.
- [5] E. F. Martini, Frederic H.; Nath, Judi L.; Bartholomew, *Fundamentals of Anatomy & Physiology*, 9th editio. San Francisco: Pearson Benjamin Cummings, 2010.
- [6] J. Fernandes, Paulo R; Folgado, "Bone Tissue Mechanics - Material Properties of Cortical Bone - Class slides," 2011.
- [7] A. Liedert, D. Kaspar, P. Augat, A. Ignatius, and L. Claes, "Mechanobiology of Bone Tissue and Bone Cells," *Mechanosensitivity in Cells and Tissues*, pp. 1–10, 2005.
- [8] "Femur by Enrique A Femur Model from 3D Scan file." [Online]. Available: <https://grabcad.com/library/femur--1>. [Accessed: 30-Mar-2017].
- [9] J. F. Hawkins, "Surgical technique;," pp. 61–62.
- [10] Y. Watanabe, N. Shiba, S. Matsuo, F. Higuchi, Y. Tagawa, and A. Inoue, "Biomechanical study of the resurfacing hip arthroplasty," *J. Arthroplasty*, vol. 15, no. 4, pp. 505–511, 2000.
- [11] M. B. Ferreira, Bárbara; Sobreiro, Ana Margarida; Marques, "ESTUDO DA REABSORÇÃO ÓSSEA DO FÉMUR NUMA ARTROPLASTIA TOTAL DA ANCA," 2017.



## VIII. Appendix

### A. MATLAB® implementations of the Huiskes' model for bone remodelling

#### A.1. Script for the intact bone: bone.m

```
%% Inputs and initial conditions:

niter = input ('number of iterations?') %maximum number of iterations
step = input ('step?')
k=input('k?')
s=input('s?')
nodes=31502;
dens= 0.3 * ones(nodes,1); %initial densities
previousdens=zeros(nodes,1);

%% Loop in the iterative process:

tic %starts counting time

for iter=1:niter
    disp(' ');
    disp(sprintf('Iteração %g',iter));

    %verify convergence condition
    averagediff=mean(abs(dens-previousdens))
    if abs(averagediff)<10^-3
        break; % stopps the loop if the convergence is verified
    else
        previousdens=dens; %updates previous densities matrix
    end

    %write the densities' file '.dat' with the data within dens matrix
    fich=fopen('dens.dat','w');
    for i=1:nodes
        fprintf(fich,'FemurModel3D-1.%d, %f\r\n',i,dens(i));
    end;
    fclose(fich);

    %Initialize ABAQUS, run Job with conditions given in INP file
    system('abaqus job=bone inter');

    %Get strain energies from ABAQUS, generating RPT file for each step
    system('abaqus viewer noGUI=andar.py');
    system('abaqus viewer noGUI=escadas.py');

    %Open strain energy densities file for the gait load, RPT file
    fich = fopen('andar.rpt');

    %initialize tline for the next cicle
    tline = fgetl(fich);
```

```

    %Detection of the line wich contains the name of the part
    while strcmp(tline, 'Field Output reported at nodes for part:
FEMURMODEL3D-1')==0
        tline = fgetl(fich);
    end

    %go to the beginig of the data
    for i=1:1:7
        fgetl(fich);
    end

    %Read and save data from RPT file
    dados=(fscanf(fich, '%g %g', [2 inf]))';

    %Close RPT file
    fclose(fich);

    %Save the nodal energy in matrix ener1
    ener1=dados(1:length(dados),2);

    %Open strain energy densities file for the climbing stairs load, RPT
file
    fich = fopen('escadas.rpt');

    %initialize tline for the next cicle
    tline = fgetl(fich);

    %Detection of the line wich contains the name of the part
    while strcmp(tline, 'Field Output reported at nodes for part:
FEMURMODEL3D-1')==0
        tline = fgetl(fich);
    end

    %go to the beginig of the data
    for i=1:1:7
        fgetl(fich);
    end

    %Read and save data from RPT file
    dados=(fscanf(fich, '%g %g', [2 inf]))';

    %Close RPT file
    fclose(fich);

    %Save the nodal energy in matrix ener2
    ener2=dados(1:length(dados),2);

    %Applies the mean to the energies matrices, merging the results from
the two loading cases
    ener=(ener1+ener2)/2;

    %Applies the Huiskes' model to the energies results, updating the dens
matrix
    for i=1:nodes
        if ener(i)/dens(i)<(1-s)*(k)

```

```

        dens(i)=dens(i)+step*(ener(i)/dens(i)-(1-s)*k);
    else if ener(i)/dens(i)>(1+s)*(k)
        dens(i)=dens(i)+step*(ener(i)/dens(i)-(1+s)*k);
    end;
end;
if dens(i)>1.74
    dens(i)=1.74; %maximum bone density
end
if dens(i)<0.01;
    dens(i)=0.01; %minimum bone density
end
end;
toc; %shows time spent after the loop began
end

%plays a chirp tone when the loop ends
load chirp
sound(y,1/2*Fs)

```

## A.2. Script for bone with implant: prosthesis.m

```

%% Inputs and initial conditions:

niter = input('number of iterations?') %maximum number of iterations
step = input('step?')
k=input('k?')
s=input('s?')
nodes=44675;
dens= 0.3 * ones(nodes,1); %initial densities
previousdens=zeros(nodes,1);

%% Loop in the iterative process:

tic %starts counting time

for iter=1:niter
    disp(' ');
    disp(sprintf('Iteração %g',iter));

    %verify convergence condition
    averagediff=mean(abs(dens-previousdens))
    if abs(averagediff)<10^-3
        break; % stops the loop if the convergence is verified
    else
        previousdens=dens; %updates previous densities matrix
    end

    %write the densities' file '.dat' with the data within dens matrix
    fich=fopen('dens.dat','w');
    for i=1:nodes
        fprintf(fich,'comprotese-1.%d, %f\r\n',i,dens(i));
    end;
    fclose(fich);

    %Initialize ABAQUS, run Job with conditions given in INP file
    system('abaqus job=prosthesis inter');

```

```

%Get strain energies from ABAQUS, generating RPT file for each step
system('abaqus viewer noGUI=andar.py');
system('abaqus viewer noGUI=escadas.py');

%Open strain energy densities file for the gait load, RPT file
fich = fopen('andar.rpt');

%initialize tline for the next cycle
tline = fgetl(fich);

%Detection of the line which contains the name of the part
while strcmp(tline, 'Field Output reported at nodes for region:
COMPOTESE-1.Region_2')==0
    tline = fgetl(fich);
end

%go to the beginning of the data
for i=1:1:7
    fgetl(fich);
end

%Read and save data from RPT file
dados1=(fscanf(fich, '%g %g', [2 inf]))';

%Close RPT file
fclose(fich);

%Open strain energy densities file for the climbing stairs load, RPT
file
fich = fopen('escadas.rpt');

%initialize tline for the next cycle
tline = fgetl(fich);

%Detection of the line which contains the name of the part
while strcmp(tline, 'Field Output reported at nodes for region:
COMPOTESE-1.Region_2')==0
    tline = fgetl(fich);
end

%go to the beginning of the data
for i=1:1:7
    fgetl(fich);
end

%Read and save data from RPT file
dados2=(fscanf(fich, '%g %g', [2 inf]))';

%Close RPT file
fclose(fich);

%Applies the mean to the energies matrices, merging the results from
the two loading cases
%Saves the number of each node and its nodal energy in matrix ener
ener=dados1;
ener(:,2)=(dados1(:,2)+dados2(:,2))/2;

```

```

    %Applies the Huiskes' model to the energies results, updating the dens
matrix
    %Verifies the number of the node, to update only the density of bone
nodes
    j=1;
    for i=1:nodes
        if ener(j,1)==i
            if ener(j,2)/dens(i)<(1-s)*(k)
                dens(i)=dens(i)+step*(ener(j,2)/dens(i)-(1-s)*k);
            else if ener(j,2)/dens(i)>(1+s)*(k)
                dens(i)=dens(i)+step*(ener(j,2)/dens(i)-(1+s)*k);
            end;
        end;
        if dens(i)>1.74
            dens(i)=1.74; %maximum bone density
        end
        if dens(i)<0.01;
            dens(i)=0.01; %minimum bone density
        end
        j=j+1;
    else
        dens(i)=1.85; %sets the density of prosthesis nodes to a value
outside the range of bone densities
    end
end;
toc; %shows time spent after the loop began
end

%plays a chirp tone when the loop ends
load chirp
sound(y,1/2*Fs)

```

### A.3. Convergence of the distribution of densities for the intact bone

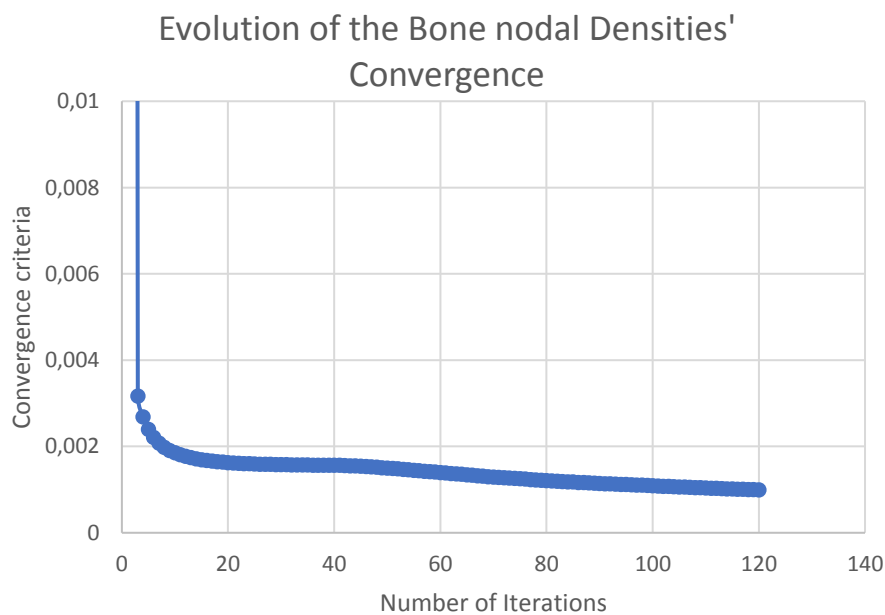


Figure VIII.A.3.1. Graphic showing the convergence of density average in all the nodes in the bone. The plot is given by the average of the absolute value of the difference between the dens and previous dens matrices.

## B. Results from simulations done for searching the Huiskes' model parameters

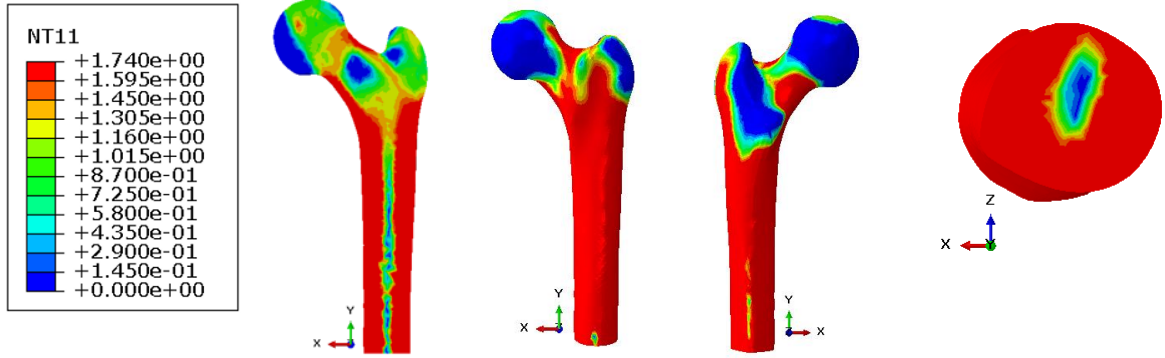


Figure VIII.B.1. These images represent bone density distribution in different cuts and views. Coronal cut in a), transversal in d) and anterior and posterior coronal planes. The parameters used are  $k=0.004$ ,  $s=0.3$ , step size=3 and initial densities=0.3 g/cm<sup>3</sup>.

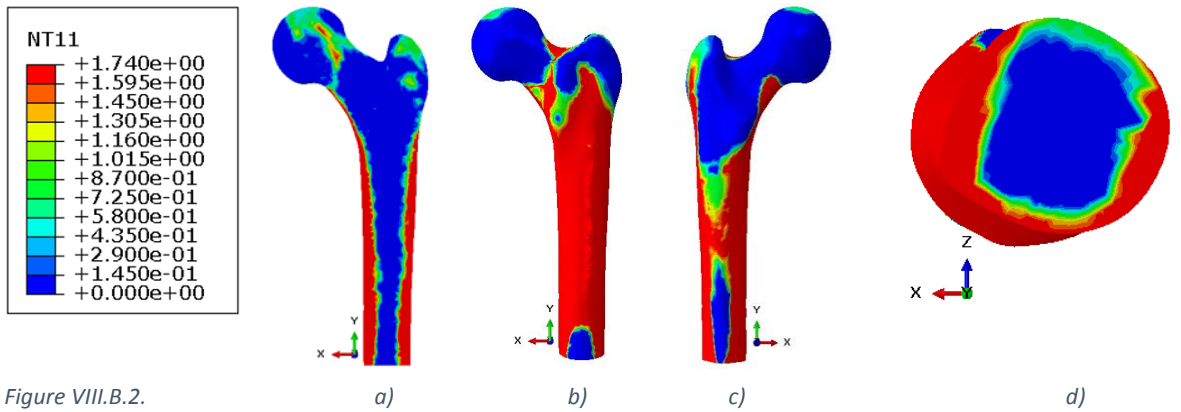


Figure VIII.B.2. These images represent bone density distribution in different cuts and views. Coronal cut in a), transversal in d) and anterior and posterior coronal planes. The parameters used are  $k=0.04$ ,  $s=0.3$ , step size=3 and initial densities=0.3 g/cm<sup>3</sup>.

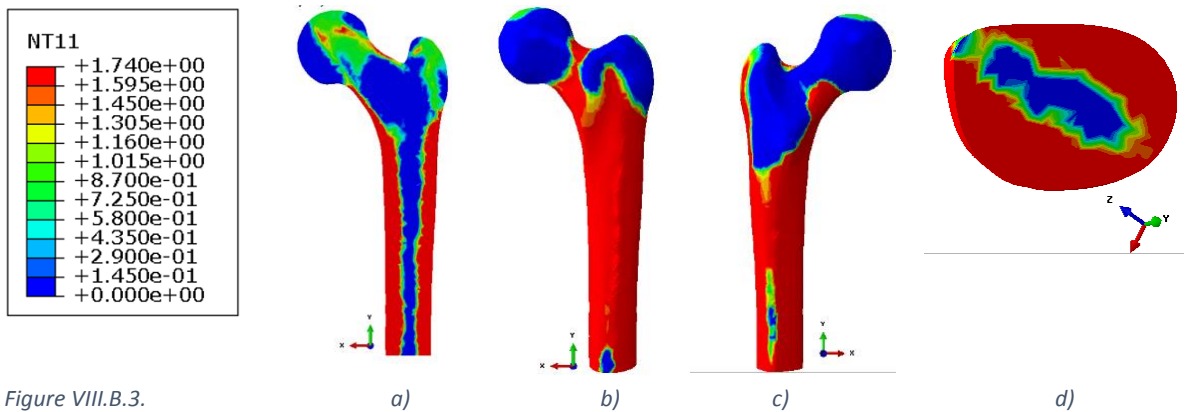


Figure VIII.B.3. These images represent bone density distribution in different cuts and views. Coronal cut in a), transversal in d) and anterior and posterior coronal planes. The parameters used are  $k=0.009$ ,  $s=0.3$ , step size=8 and initial densities=0.3 g/cm<sup>3</sup>.

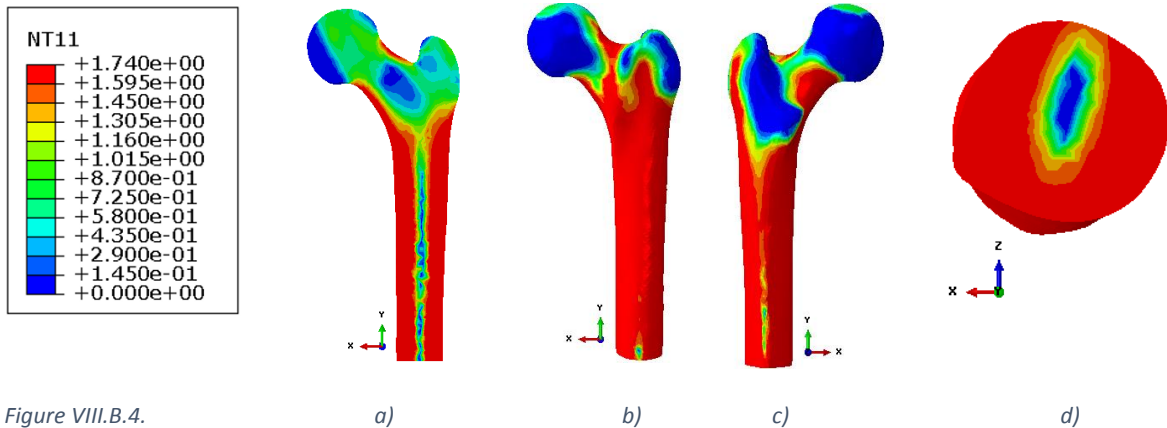


Figure VIII.B.4. These images represent bone density distribution in different cuts and views. Coronal cut in a), transversal in d) and anterior and posterior coronal planes. The parameters used are  $k=0.009$ ,  $s=0.3$ , step size=0.8 and initial densities=0.3 g/cm<sup>3</sup>.

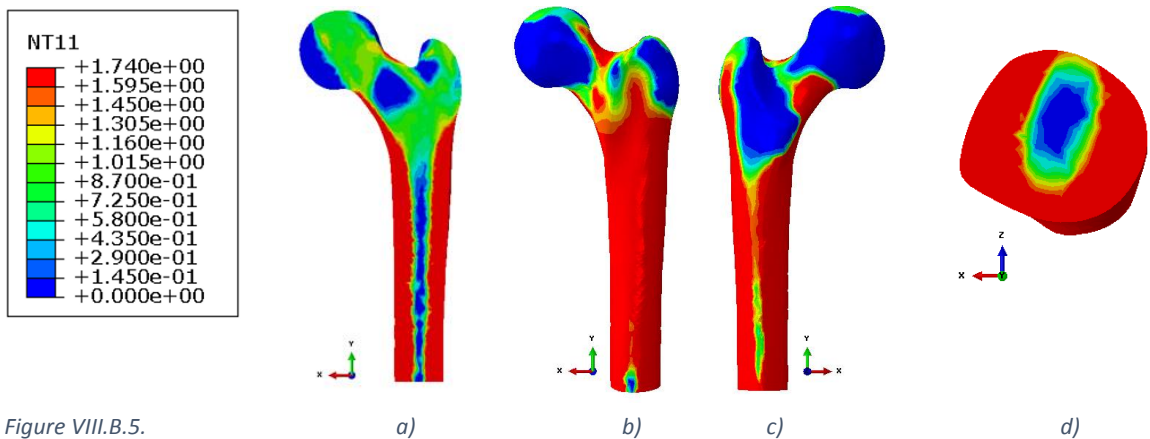


Figure VIII.B.5. These images represent bone density distribution in different cuts and views. Coronal cut in a), transversal in d) and anterior and posterior coronal planes. The parameters used are  $k=0.009$ ,  $s=0.3$ , step size=3 and initial densities=0.3 g/cm<sup>3</sup>.

### C. Results from simulations done for the different hip-resurfacing prosthesis' materials

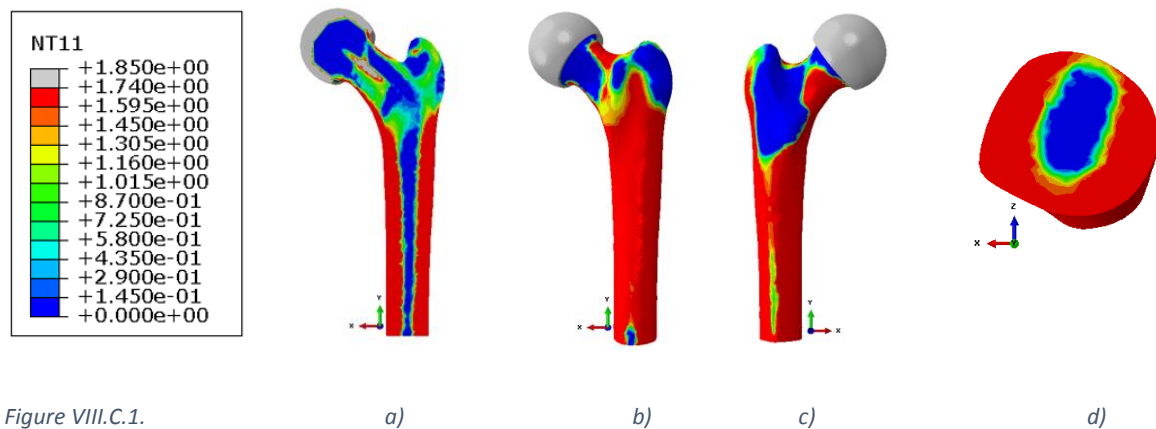
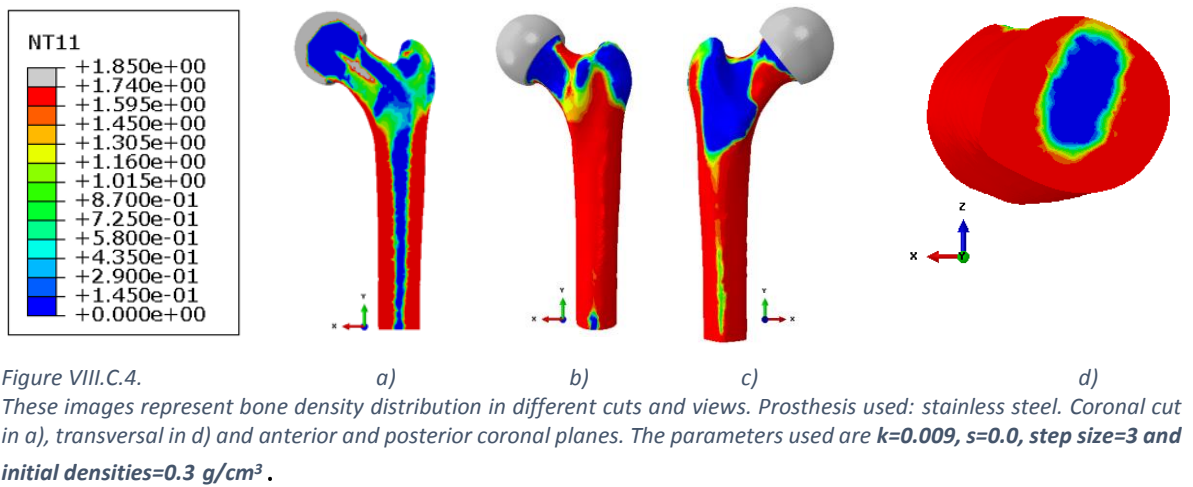
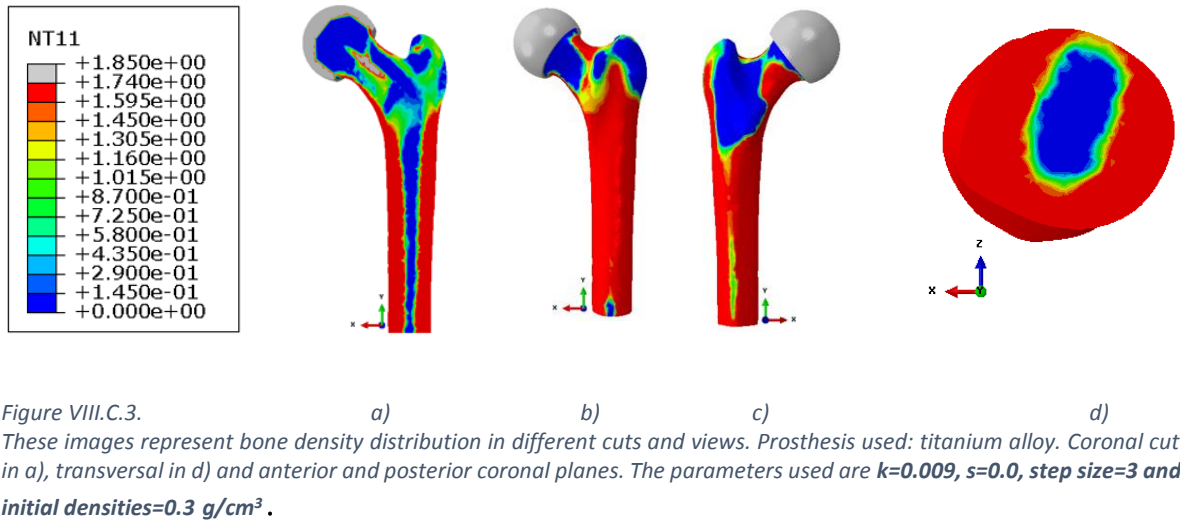
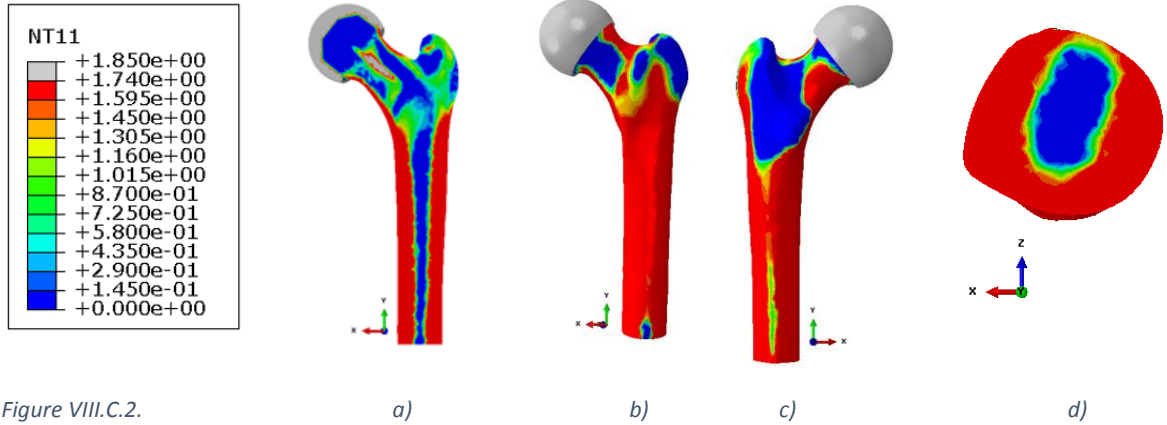


Figure VIII.C.1. These images represent bone density distribution in different cuts and views. Prosthesis used: Co-Cr. Coronal cut in a), transversal in d) and anterior and posterior coronal planes. The parameters used are  $k=0.009$ ,  $s=0.0$ , step size=3 and initial densities=0.3 g/cm<sup>3</sup>.





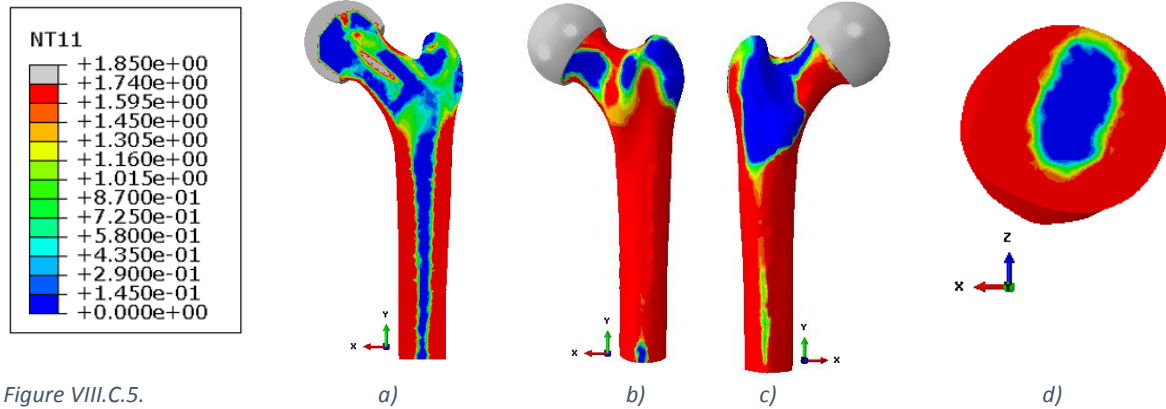


Figure VIII.C.5. These images represent bone density distribution in different cuts and views. Prosthesis used:  $E=3$  GPa. Coronal cut in a), transversal in d) and anterior and posterior coronal planes. The parameters used are  $k=0.009$ ,  $s=0.0$ , step size=3 and initial densities=0.3 g/cm<sup>3</sup>.

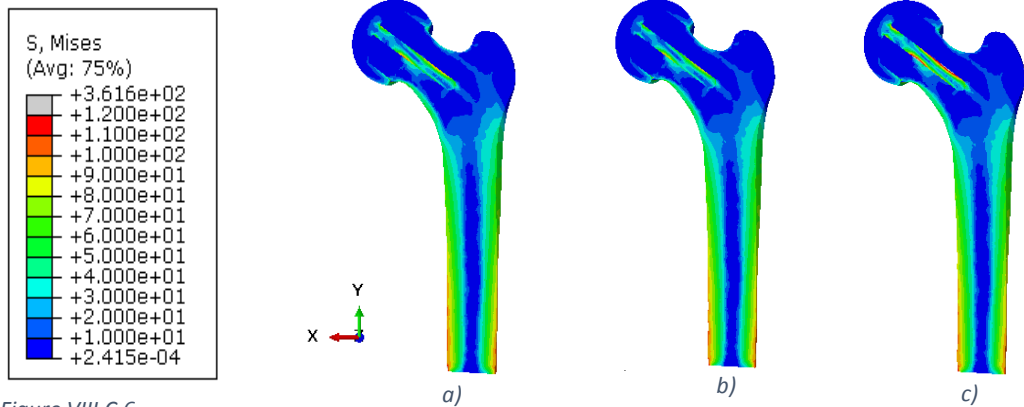


Figure VIII.C.6 Representation of the von Mises stresses, loading case "gate", for the femur with an implant made of a) Co-Cr, b) titanium and c) stainless steel.

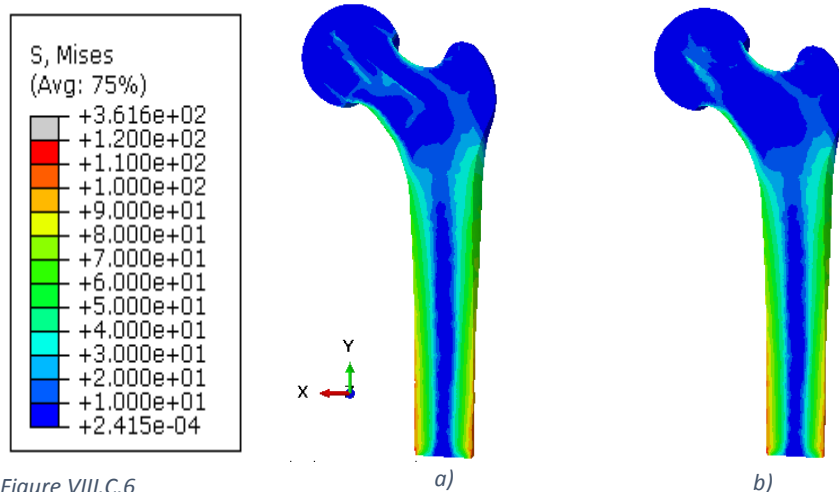
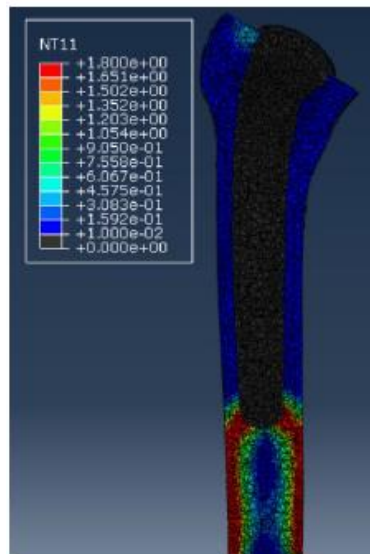


Figure VIII.C.6 Representation of the von Mises stresses, loading case "gate", for the femur with an implant, which material has a Young's modulus of a) 17 GPa, b) 3 GPa.

#### D. Results from colleagues for comparison



*Figure VIII.D.1. Density distribution for femur with a prosthesis of Co-Cr implanted. It is representative of a stress shielding phenomenon. [11]*